

# **FFI RAPPORT**

## **PENETRATION INTO MODULAR TARGETS**

OLSEN Åge Andreas Falnes, SJØL Henrik, TELAND Jan Arild

**FFI/RAPPORT-2001/05787**



FFIBM/766/130

Approved  
Kjeller 12. December 2002

Bjarne Haugstad  
Director of Research

## **PENETRATION INTO MODULAR TARGETS**

OLSEN Åge Andreas Falnes, SJØL Henrik, TELAND  
Jan Arild

FFI/RAPPORT-2001/05787

**FORSVARETS FORSKNINGSINSTITUTT**  
**Norwegian Defence Research Establishment**  
P O Box 25, NO-2027 Kjeller, Norway



**FORSVARETS FORSKNINGSIINSTITUTT (FFI)**  
**Norwegian Defence Research Establishment**

**UNCLASSIFIED**

P O BOX 25  
 NO-2027 KJELLER, NORWAY  
**REPORT DOCUMENTATION PAGE**

**SECURITY CLASSIFICATION OF THIS PAGE**  
 (when data entered)

1) PUBL/REPORT NUMBER  FFI/RAPPORT-2001/05787	2) SECURITY CLASSIFICATION  UNCLASSIFIED	3) NUMBER OF PAGES  26
1a) PROJECT REFERENCE  FFIBM/766/130	2a) DECLASSIFICATION/DOWNGRADING SCHEDULE  -	
4) TITLE  PENETRATION INTO MODULAR TARGETS		
5) NAMES OF AUTHOR(S) IN FULL (surname first) OLSEN Åge Andreas Falnes, SJØL Henrik, TELAND Jan Arild		
6) DISTRIBUTION STATEMENT Approved for public release. Distribution unlimited. (Offentlig tilgjengelig)		
7) INDEXING TERMS IN ENGLISH:		IN NORWEGIAN:
a) Modular targets	b) Concrete	c) Autodyn
d) Penetration	e)	f) Penetrasjon
THESSAURUS REFERENCE:		
8) ABSTRACT  Penetration into modular targets (i.e. a wall or similar structure consisting of several target blocks) is examined using a variety of methods. Full Autodyn-3D simulations are performed and supported by analytical calculations. Both corner impacts (near the edge of a block) and joint impacts (at the intersection between blocks) are considered.  It is found that the penetration depth may increase considerably in both cases, although in certain situations the projectile may be deflected away from the target. It is recommended that the gap between the various modules should be as little as possible, in which case it is seen that boundary effects will be negligible.  In a real design, the probability of a direct hit exactly at a joint will be quite low. Furthermore, adjacent modules will often have to be fixed to each other by some mechanical means, which can offer some additional protection. These issues should be included in a design of modular protection measures.		
9) DATE  12. December 2002	AUTHORIZED BY  This page only  Bjarne Haugstad	POSITION  Director of Research

ISBN-82-464-0736-8

**UNCLASSIFIED**

**SECURITY CLASSIFICATION OF THIS PAGE**  
 (when data entered)



## CONTENTS

	Page
1      INTRODUCTION	7
2      SIMULATIONS	8
2.1    Projectile	9
2.2    Target	9
2.3    Center impact	10
2.4    Joint impacts	10
2.5    Corner impacts	10
2.6    Discussion and summary of results	11
3      THEORETICAL CONSIDERATIONS	12
3.1    Material data for analytical calculations	12
3.2    Corner impacts	12
3.3    Joint impacts	14
3.4    Conclusions from the semi-analytical approach	15
4      PREVIOUS WORK ON RELATED PROBLEMS	15
4.1    Layered targets	16
4.2    Perforation	17
5      CONCLUSIONS	17
References	18
A      CONCRETE DATA	19
B      STEEL DATA	20
C      ANALYTICAL METHOD FOR JOINT IMPACTS	20
D      THE <i>MATHEMATICA</i> ROUTINE	22
Distribution list	26



## PENETRATION INTO MODULAR TARGETS

### 1 INTRODUCTION

In the Swedish-Norwegian project on “High Performance Concrete” (HPC), the potential use of HPC in protective structures was examined. The penetration resistance of HPC compared to standard concrete was analysed by experimental work, numerical analysis and some theoretical considerations.

Concrete structures are widely used as protection in permanent structures for two major reasons: Concrete works reasonably well against several different types of ammunition and is a low cost, commercially available material. High cost-effectiveness is also a property of some types of HPC.

The high cost effectiveness of concrete has generated an interest in utilizing the material in field locations as temporary protective shields. In order to achieve this, one may build walls from pre-cast blocks, a bit like building Lego with giant pieces. Figure 1.1 shows a sketch of such a wall made up of three concrete modules. The individual pieces should be possible to handle with standard logistics equipment.

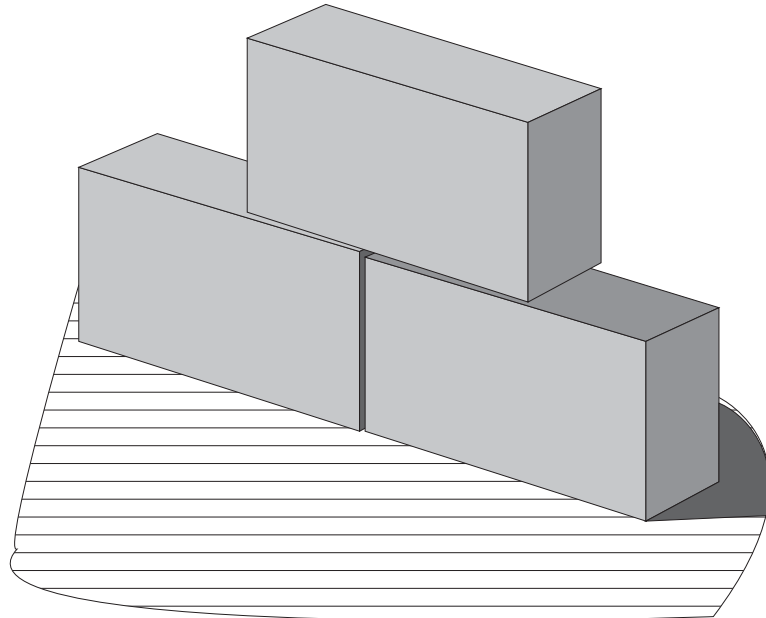


*Figure 1.1 A modular wall consisting of three concrete blocks.*

The joints in such a modular wall are potential weak spots, possibly resulting in a lower protection level than provided by a continuously cast structure. For example, it was seen in (1)-(2) that for small unconfined targets, boundary effects led to increased penetration depths. However, the free surface theory is not directly applicable in our case since the material is

slightly confined. The problem is further complicated by the fact that the situation is unsymmetric for impacts near a corner or one of the joints.

This report describes a first approach to analysing the situation described above. Numerical simulations and theoretical considerations have been the main methods due to lack of experimental data.

Since the problem did not exhibit geometrical symmetry, it was necessary to perform full 3D simulations, a very time consuming process. For this reason, our simulations were limited to a specific 75 mm projectile impacting a variety of 150 MPa concrete target set-ups. Thus, only very few, but relevant, examples were analysed, which means one should be rather careful in drawing general conclusions. However, some theoretical work was performed as support of the results indicated by the 3D simulations.

Despite the obvious limitations, the work should provide valuable insight into the general nature of the problem.

## 2 SIMULATIONS

In a perfect world it would have been desirable to perform a parameter study varying different parameters like target configuration, material model, impact point and velocity, but as mentioned earlier this was not possible due to time constraints. Instead we will look closely at a small number of scenarios with a large variation in boundary properties and impact position.

Before getting started, a few definitions are necessary: For want of a better word, *corner impact* means that the projectile impacts near the corner of a block with no neighbours. Similarly, by *joint impacts* we mean impacts on a joint between two or more modules. In general, we focus our attention on the worst case in which four modules are placed side by side. These cases of corner and joint impact are illustrated in Figure 2.1.

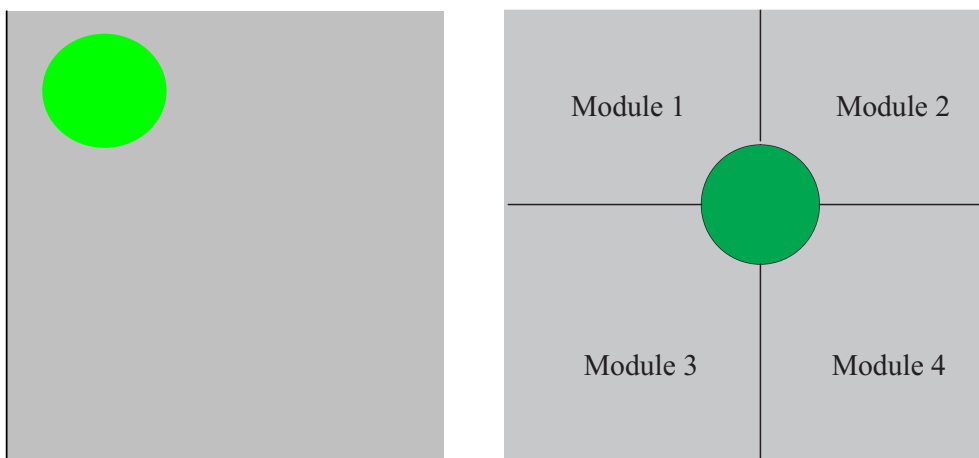


Figure 2.1 Corner impact and joint impact.

At the time of writing, the exact details of the joints in a future protection design were not clear. The uncertain aspects can be summarised by the following three points:

- The effective contact area between modules is unknown.
- The mean separation and the variance in the separation are unknown.
- The transmission properties at the joints are unknown, as well as any spatial variation of these properties.

It was considered beyond the scope of this report to investigate different designs, so in our simulations we have simply assumed that a small air-gap separates the modules.

## 2.1 Projectile

As projectile in our simulations, we have chosen a 75 mm steel projectile that was used in many of the experiments within the HPC-project. Since the projectile remains undeformed, the choice of projectile or steel model should not have a major influence on the qualitative results. The projectile data are given in Table 2.1. The projectile was modelled using the Lagrangian processor in Autodyn.

*Table 2.1 Projectile data for Autodyn simulations.*

Material	4340 steel (see Appendix B)
Mass	6,32 kg
Ogive radius in nose	140 mm
Diameter	75 mm
No of cells in radius	5
Total length	225 mm

## 2.2 Target

The concrete modules in our simulations were arbitrarily chosen to be rectangular blocks of 2,50 m × 2,50 m × 1,25 m, having a mass of 21 tons. In the penetration region, the mesh consisted of cubical cells with length 10 mm.

The concrete material model included a porous equation of state, a pressure dependent yield surface (incorrectly called Mohr-Coulomb in Autodyn terminology) and a tensile failure criterion. The values of the input parameters were found by scaling a 200 MPa concrete model so that it should correspond to a concrete with compressive strength of 150 MPa. Numerical values of the material model parameters are tabulated in Appendix A.

Using a more sophisticated concrete model, such as the RHT model (3), might have improved the accuracy of the results compared to the experiments. However, at the time of simulating, the RHT model was not incorporated into the Autodyn-3D material library and we also lacked experimental input data to the model for this particular concrete. The qualitative results obtained should, as mentioned earlier, not be affected by the use of a simple Mohr-Coulomb model.

Further, it must be remembered that we are mainly interested in the relative behaviour for different impact situations, more than the exact behaviour (although the latter would of course be welcome, if it could be achieved within a reasonable period of time). The lack of sophisticated material model should therefore not be a problem.

### 2.3 Center impact

For comparison, we first looked at center impact on a target that was large enough for boundary effects to be excluded. A penetration depth of 278 mm was then obtained. The question is now how much this will increase for the joint and corner impact scenarios.

### 2.4 Joint impacts

A major concern is that no information is available on the coupling between the individual blocks, and hence the behaviour of stress waves crossing the boundaries. We have for this reason looked at two joint impact scenarios where the separation between the blocks was 1 mm and 5 mm, respectively. The results for penetration depth are tabulated in Table 2.2.

*Table 2.2 The penetration depths of the projectile in the joint impact simulations.*

Simulation	Penetration depth	Time of process
Joint impact, 5 mm spacing	390 mm	1,4 ms
Joint impact, 1 mm spacing	290 mm	1,1 ms

We note that there is a large difference between a 1 mm and a 5 mm module spacing. In fact, the penetration depth increases by about out 35%. On considering the geometry, this is hardly a surprising result. When the gap between the blocks decreases, in addition to increasing the area of material which does work on the projectile, the confining effect is also larger. This results in an increased yield strength for the target material, which is also to a greater extent forced to stay in place instead of being pushed away.

### 2.5 Corner impacts

Next, we considered two different corner impact situations, corresponding to different levels of confinement. In the first case the surface was completely free, whereas in the other situation it was slightly constrained by a large block 5 mm away. Figure 2.2 shows the final state of these two simulations.

The free surface turned out to induce such a large asymmetry in the force on the projectile, that it obtained a deflection as well as a rotation resulting in yaw. As a consequence, the projectile was deflected away and actually exited the target at 383 mm in the z-direction at  $t= 0.9$  ms. Without any constraints on the surfaces of the module, most of the cells failed and there were no mechanical forces to prevent the motion of the material.

It turned out that putting a second block 5 mm away was sufficient to keep the projectile inside the original target. In the confined situation, we obtained a penetration depth of 344 mm after 1.9 ms.

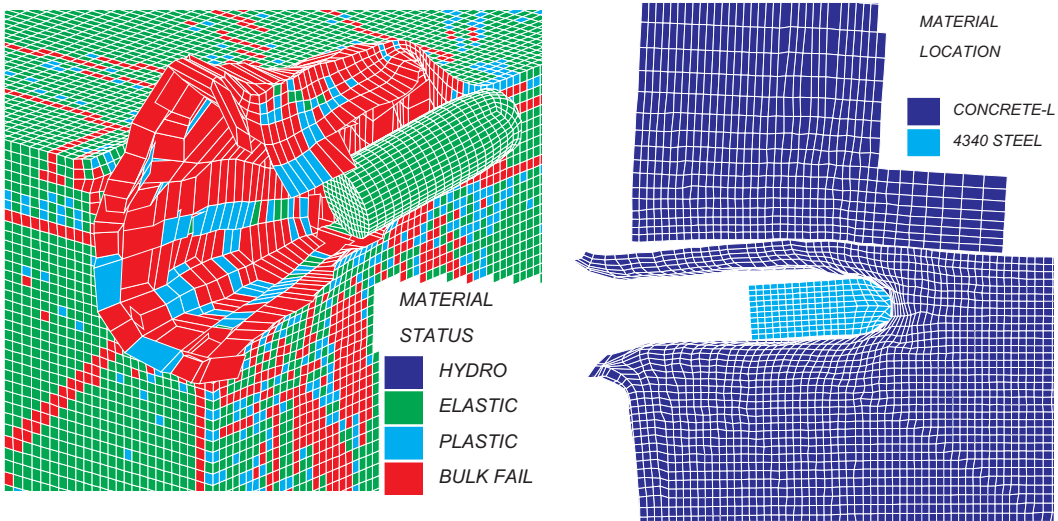


*Figure 2.2 Two simulations of a corner impact. The left panel shows the situation for a free surface, while in the other case the modules are constrained by a large concrete block 5 mm away.*

## 2.6 Discussion and summary of results

On reviewing the results, there is seen to be a significant increase in penetration depth for both the “joint impact” and “corner impact” situations, compared with a semi-infinite target. However, the magnitude of the increase depends strongly on the separation of the individual blocks. Thus, in a real situation it is very important to pack the blocks as tightly as possible.

Ideally, we would have liked to perform a 3D parameter study to assess how these results depended on the target material parameters, but this was impossible given the limited time frame. However, earlier work (1,2) in 2D gives us some indications about what would have happened. Probably the results would have been strongly dependent on the value of the tensile failure limit. For a lower tensile limit, i.e. the material fails more easily, the increase in penetration depth would have been even more dramatic as a function of the gap size, whereas for a higher tensile limit the effect would have been less.

It is also interesting to compare the simulation results with some experiments performed in 1999 at Bofors in Sweden (4), which gave penetration depths between 450 mm and 540 mm for the central impact case. This is quite a lot more than obtained in the simulations, which indicates that our target material model is not very similar to the concrete used in those experiments. Unfortunately, no material tests were performed on that particular concrete, so accurate input data were not available, and as mentioned, we only arrived at our concrete model by scaling down the strength of a completely different concrete. However, since the material model contains the same deficiencies in all our simulations, including the corner impacts, it is not unreasonable to conclude that the relative increase we see in penetration depth reflects the relative increase we would have seen experimentally.

### 3 THEORETICAL CONSIDERATIONS

Due to the long duration of a full 3D-simulation, we were in the previous chapter unable to perform a sensitivity study on how the penetration process depends on distance from the impact point to the target boundary. However, a combined numerical and analytical method has been developed (6,7) which significantly reduces the CPU-time, although at the expense of accuracy.

The general idea behind this approach is to remove the target mesh completely and simulate the effect of the target mesh by imposing a pressure boundary condition on the projectile. The magnitude of the pressure  $p_r(v)$  is then calculated from analytical penetration theory (5). For further details about this approach, the reader is referred to (6) and (7).

#### 3.1 Material data for analytical calculations

Since the target is described analytically, it is not possible to apply the most advanced material models for the target material. In this case we have used a simple Mises material model with parameter values given in Table 3.1. For the constant yield stress we have chosen a value close to the maximum yield stress of the Mohr-Coulomb yield surface used in the Autodyn simulations (Appendix A). Note that there is no tensile failure in the model.

*Table 3.1 Concrete data used in the combined analytical and numerical approach.*

Poisson ratio, $\nu$	Shear modulus, $G$	Density, $\rho$	Yield strength, $Y$
0.25	$2.5 \cdot 10^4$ MPa	2700 kg/m <sup>3</sup>	300 MPa

#### 3.2 Corner impacts

In the corner impact situation, we are now able to conduct a sensitivity study to see how the behaviour of the projectile depends on the position of the impact point. Some of the situations considered are depicted in Figure 3.1, where the distance  $d_{initial}$  denotes the shortest distance between the projectile nose and the target edge at time  $t=0$ .

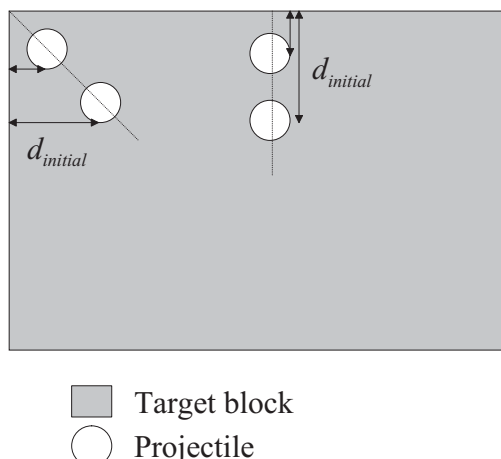


*Figure 3.1 Some of the impact points considered.*

The coordinate system is chosen so that the origin coincides with the tip of projectile nose at the time of impact, and the z-axis is pointing along the projectile axis in the same direction as the projectile.

The asymmetric forces on the projectile leads to a curved trajectory inside the target. Obviously this means that the actual distance the projectile travels is longer than the z-component of the path length. In terms of threat, the z-component is the most interesting quantity, but the total length of the penetration channel is more closely related to the actual force reduction. However, it will be seen that the same trend is observed in both cases.

The results of the calculations are presented in Table 3.2 and Figure 3.2. When the projectile exits the target, only the approximate z-value is given (the x- and y-values should then be identical to  $d_{initial}$  – see above definition of coordinate system).

Generally, it is clearly seen that the penetration depth increases for impacts near the block surfaces. However, the penetration depth seems to converge quickly to the value expected in a semi-infinite target. Already at an initial distance  $d_{initial}$  of 4-5 projectile diameters the penetration depth is close to the value in an infinite target for the corner impacts. This is probably a consequence of our concrete not having a tensile failure model implemented. As expected, the boundary effects are even weaker for side impacts.

*Table 3.2 The final position ( $x,y,z$ ) of the projectile tip, and the penetration depth  $z_0$ , for a number of numerical calculations for impacts near a free surface.*

Simulation	$\frac{d_{initial}}{2a}$	$x$ (mm)	$y$ (mm)	$z$ (mm)	Length of penetration channel $z_0$ (mm)
Corner	1	-	-	235,1	Exits target at indicated position
Corner	1,5	-	-	322,9	Exits target at indicated position
Corner	2	92,5	114,7	413,3	458,6
Corner	3	8,6	13,6	349,3	351,7
Corner	4	2,3	6,4	338,9	341,0
Corner	6	-0,2	3,6	334,3	336,3
Corner	12	-1,4	2,7	332,3	334,3
Corner	Center	-1,5	2,4	331,9	333,9
Side	1	-	-	207,6	Exits target at indicated position
Side	2	-4,1	67,5	365,7	376,6
Side	3	-2,2	14,1	340,7	343,1
Side	4	-1,9	6,8	335,5	337,6
Side	6	-1,6	3,9	333,1	335,1
Side	12	-1,6	2,7	332,1	334,1
Side	Center	-1,5	2,4	331,9	333,9

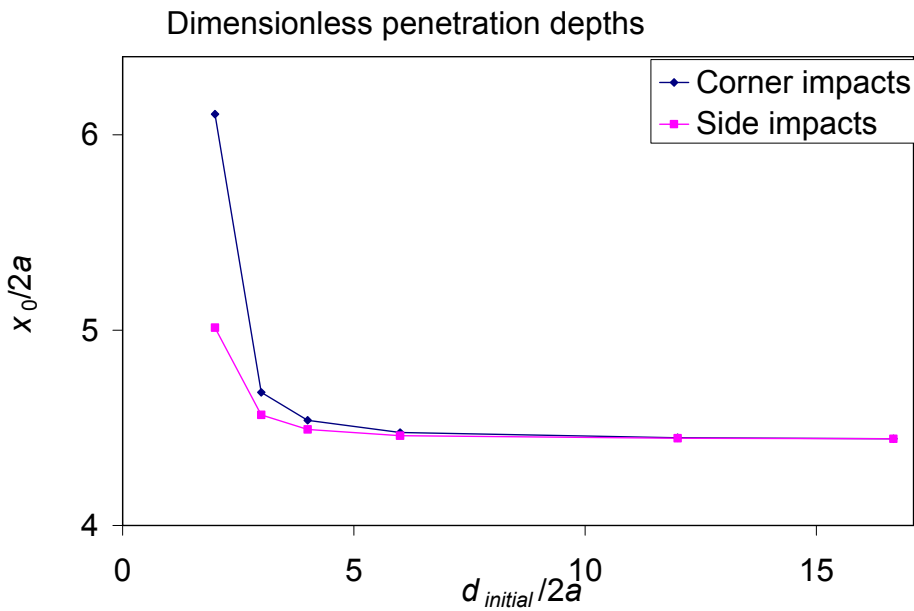


Figure 3.2 The penetration depth with free surface effects for those cases where the projectile remains inside the target.

### 3.3 Joint impacts

For the joint impact case, it is unfortunately not possible to use the same approach as for corner impacts. Instead we will try a purely analytical approach.

Figure 3.4 shows a sketch of a typical impact situation. We obviously expect an increased penetration depth compared with the case of a centre impact, but several mechanisms exist that can contribute to this increase.

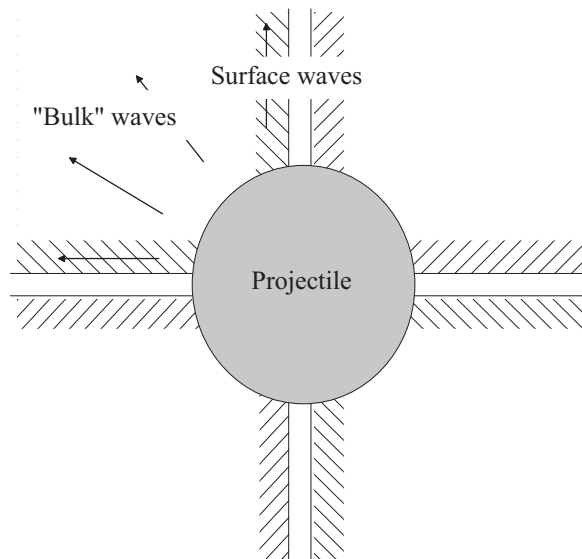


Figure 3.4 Joint impact.

First of all we have the obvious geometric effect of a smaller contact area between the projectile and the target. Secondly, fracturing and damage of the concrete could be affected by the surfaces. Finally, the density of aggregate may be lower near the surfaces than inside,

thereby weakening the concrete. In this section we will focus only on the geometric effects, which means boundary effects will probably be underestimated.

In (8) the penetration problem was solved for the slightly different geometry of the target containing a pre-drilled cavity. This was done by integrating the force only over the region where the projectile nose was in contact with the target. The same idea can be used here, but with other integration limits. Results for the three cases of 0, 1 and 5 mm spacing, respectively, are shown in Table 3.3 for both the analytical calculation and the previous Autodyn simulations. Details about the analytical approach are given in Appendix C.

*Table 3.3 Penetration depths from the analytical calculations and Autodyn simulations.*

Separation between modules	Penetration depth $x$ , Autodyn	Penetration depth $x$ , theory	$\frac{x}{x_0}$ (sim)	$\frac{x}{x_0}$ (theory)
0 mm	278 mm	330 mm	1,00	1,00
1 mm	290 mm	341 mm	1,04	1,03
5 mm	390 mm	392 mm	1,40	1,19

There is seen to be a larger difference between the 0 mm and 5 mm spacing for the Autodyn simulations than for the analytical theory. This is to be expected, since as noted earlier, only the geometrical effects have been included in the analytical theory.

### 3.4 Conclusions from the semi-analytical approach

Although the cavity expansion approach has been shown to give good results for penetration into concrete, we are facing a new challenge when dealing with finite boundaries within such a framework.

The behaviour of a material like concrete is difficult to describe analytically, as non-linear effects ranging from loading rate dependencies to discontinuities (cracks and fractures) play a role. These effects have not been accounted for in the analytical models studied in this chapter. However, it is clear that including such effects would have increased the boundary effects. Consequently the results of the simplified models in this chapter must be considered as conservative. Still, the results from the analytical approach are seen to support our conclusion from the simulation chapter, that care should be taken to minimize the gaps between the various modules.

## 4 PREVIOUS WORK ON RELATED PROBLEMS

Because of the many uncertainties in the analytical and numerical approaches, it would be useful to validate our results against previous work, preferably experiments. Unfortunately, to our knowledge, no directly relevant experiments have been conducted on modular targets to date. On the other hand, previous work has been carried out that involve boundary effects. In this section we briefly look at two sets of experiments that bear some relevance to our present work.

#### 4.1 Layered targets

By layered targets, we mean a number of individual plates stacked behind each other.

We first look at a series of experiments with the 75 mm projectile in Bofors 1997. In Table 4.1 and Table 4.2, the penetration depth into layered targets and homogenous targets are compared, where relevant information is available.

*Table 4.1 Experiments with 75 mm projectile, from experiments at Bofors in 1997  
Complete data can be found in (1).*

	Shot nr	Plate Thickness	Compressive strength [MPa]	Impact Velocity [m/s]	Penetration depth [mm]
Layered	97-1	10 x 200 mm	38	484	680
Solid	97-3	2000 mm	38	480	655
Solid	97-4	2000 mm	38	483	660
Layered	97-2	5 x 200 mm	200	480	200
Solid	97-5	1000 mm	180	485	250
Solid	97-6	1000 mm	180	489	235
Solid	97-7	500 mm	180	485	240

If the boundaries between the layers could be regarded as free boundaries, we would expect the penetration depth to increase in the layered targets compared with the homogeneous ones. However, we see from Table 4.1 that the experiments are inconclusive on this issue. The shots on 38 MPa concrete show a small increase in penetration depth in the layered targets. On the other hand, the shots on harder concrete (HPC) show the opposite trend: the penetration depth into homogenous targets was approximately 20% larger than into a layered target. The difference in compressive strength can not fully explain this surprising observation. According to Forrestal's formula (9), the penetration depth into 180 MPa targets should be approximately 9% larger compared to 200 MPa targets.

*Table 4.2 FFI-experiments with flat 12 mm projectile (10).*

	Shot nr	Plate thickness	Compressive strength [MPa]	Impact velocity [m/s]	Penetration depth [mm]
Layered	4	5 x 40 mm	35	1366	120
Layered	5	5 x 40 mm	35	1355	100
Solid	6	200 mm	35	1401	100
Solid	7	200 mm	35	1366	90
Layered	15	5 x 40 mm	35	935	50
Solid	14	200 mm	35	1016	60
Layered	16	5 x 40 mm	35	1370	80
Solid	13	200 mm	35	1361	88

Experiments at FFI (10) with flat nose 12 mm projectiles, as shown in Table 4.2, showed no significant difference in penetration resistance between layered and homogenous targets.

Clearly the experiments indicate that there is little difference in penetration depth for layered and homogenous targets. The obvious conclusion from the results is that provided the layers are in contact with each other, the boundaries between individual layers do not behave like a free surface. In fact, a better model seems to be to ignore them completely and calculate the penetration depth as if the target was homogeneous. It is difficult to see why this should not carry over to modular targets, provided that the modules are packed close together. This is in good agreement with both our simulations and semi-analytical work, which found little difference between a 1 mm and 0 mm separation.

## 4.2 Perforation

Perforation of concrete targets is also a boundary effect problem. In (11) this problem was investigated analytically using the cavity expansion method and compared with various experimental data. The general impression was that the cavity expansion approach gives very reasonable results, despite the simple material models used. This possibly suggests that a sophisticated material model might not be necessary to obtain good predictions, and that even the results in this report may be more accurate than first imagined. However, this may not be true in general, so care must be taken when interpreting such results.

## 5 CONCLUSIONS

In this report we have made an initial attempt to analyse the effect of penetration into a modular target by considering modules separated by an air gap. Selected 3D hydrocode simulations as well as semi-analytical methods were used as tools. It is clear that each method has limitations for describing such complicated impact processes, and our results have been based on the use of very simple material models.

Impacts near the module surfaces have been our main interest. It has been seen that even small gaps between the modules can degrade the protection level significantly, while closely spaced modules behave nearly as a solid material. This was seen both in the simulations, the analytical theory and in earlier experiments on layered concrete targets.

In a real design, the probability of being hit exactly at a joint will be quite low. Furthermore, adjacent modules will often have to be fixed to each other by some mechanical means which can offer some protection.

Possible further work in this field may include:

- Improving the semi-analytical models. A first step is to include the boundary impedance and try to quantify it.
- Achieving more realistic results from the hydrocodes by using smaller cells and more advanced material models .
- Performing further experiments on actual designs against specific threats.

## References

- (1) Teland J A, Sjøl H, "Boundary effects in penetration into concrete", FFI/RAPPORT-2000/05414, 2000
- (2) Sjøl H, Teland J A, "Boundary effects in penetration of rigid projectiles into "High Performance Concrete" (HPC) Targets", Proceedings from the 10<sup>th</sup> international symposium on interaction of the effects of munitions with structures, San Diego, USA, 7. – 11. May 2001
- (3) Riedel W, "Beton unter dynamischen Lasten. Meso- und makromechanische Modelle und ihre Parameter", EMI-Bericht 6/00, 2000
- (4) Magnusson J, Unosson M, Carlberg A, "High Performance Concrete "HPC", Field Experiments and Production", FOI-report FOI-R-0256-SE, 2001
- (5) Teland J A, "A Review of Analytical Penetration Mechanics", FFI/RAPPORT-99/01264, 1999
- (6) Warren T L, Poormon K L, Int J. Impact Engng Vol 25, 2001, pp. 993-1022
- (7) Olsen Å A F, Teland J A, "Quick and Easy Autodyn 3D Simulations", FFI/RAPPORT-2002/00575, 2002
- (8) Teland J A, "A First Approach to Penetration of Tandem Charges into Concrete", FFI/RAPPORT-2001/00624, 2001
- (9) Forrestal M J, Altman B S, Cargile J D, Hanchak S J, "An empirical equation for penetration depth of ogive-nose projectiles into concrete targets", Int. J. Impact Eng. Vol 15, pp 395-405, 1994
- (10) Sjøl H, Teland J A, Kaldheim Ø, "Penetrasjon i betong med 12 mm prosjektiler", FFI/NOTAT-98/04392, 1998 (in Norwegian)
- (11) Sjøl H, Teland J A, "Perforation of concrete targets", FFI/RAPPORT-2001/05786, 2001

## A CONCRETE DATA

MATERIAL NAME: CONCRETE-L

EQUATION OF STATE: Porous

Reference density (g/cm3)	:	3.05000E+00
Solid Sound Speed (m/s)	:	3.00000E+03
Porous Sound Speed (#1) (m/s)	:	2.72000E+03
Density #1 (g/cm3)	:	2.70000E+00
Density #2 (g/cm3)	:	2.80000E+00
Density #3 (g/cm3)	:	2.90000E+00
Density #4 (g/cm3)	:	3.00000E+00
Density #5 (g/cm3)	:	3.10000E+00
Density #6 (g/cm3)	:	3.20000E+00
Density #7 (g/cm3)	:	3.30000E+00
Density #8 (g/cm3)	:	0.00000E+00
Density #9 (g/cm3)	:	0.00000E+00
Density #10 (g/cm3)	:	0.00000E+00
Pressure #1 (kPa)	:	1.50000E+05
Pressure #2 (kPa)	:	2.50000E+05
Pressure #3 (kPa)	:	5.00000E+05
Pressure #4 (kPa)	:	8.00000E+05
Pressure #5 (kPa)	:	1.10000E+06
Pressure #6 (kPa)	:	1.50000E+06
Pressure #7 (kPa)	:	2.00000E+06
Pressure #8 (kPa)	:	0.00000E+00
Pressure #9 (kPa)	:	0.00000E+00
Pressure #10 (kPa)	:	0.00000E+00

STRENGTH MODEL: Mohr-Coulomb

Shear Modulus (kPa)	:	2.50000E+07
Pressure #1 (kPa)	:	0.00000E+00
Pressure #2 (kPa)	:	2.50000E+04
Pressure #3 (kPa)	:	5.00000E+04
Pressure #4 (kPa)	:	1.00000E+05
Pressure #5 (kPa)	:	2.00000E+05
Pressure #6 (kPa)	:	3.00000E+05
Pressure #7 (kPa)	:	4.00000E+05
Pressure #8 (kPa)	:	6.00000E+05
Pressure #9 (kPa)	:	8.00000E+05
Pressure #10 (kPa)	:	1.00000E+06
Yield Stress #1 (kPa)	:	2.00000E+04
Yield Stress #2 (kPa)	:	1.13100E+05
Yield Stress #3 (kPa)	:	1.50900E+05
Yield Stress #4 (kPa)	:	2.02500E+05
Yield Stress #5 (kPa)	:	2.73000E+05
Yield Stress #6 (kPa)	:	3.26500E+05
Yield Stress #7 (kPa)	:	3.69300E+05
Yield Stress #8 (kPa)	:	4.41200E+05
Yield Stress #9 (kPa)	:	5.00800E+05
Yield Stress #10 (kPa)	:	5.52600E+05

FAILURE MODEL: Hydro

Hydro Tensile limit (PMIN) (kPa)	:	-1.20000E+04
Crack Softening, Gf (J/m <sup>2</sup> )	:	0.00000E+00
or, Kc (mN/m <sup>3</sup> /2)	:	0.00000E+00

EROSION MODEL: Eff. Plastic Stn.

Erosion Strain : 1.20000E+02

## B STEEL DATA

MATERIAL NAME: 4340 STEEL

EQUATION OF STATE: Linear

Reference density (g/cm <sup>3</sup> )	:	7.83000E+00
Bulk Modulus (kPa)	:	1.59000E+08
Reference Temperature (K)	:	3.00000E+02
Specific Heat (C.V.) (J/kgK)	:	4.77000E+02

STRENGTH MODEL: Johnson-Cook

Shear Modulus (kPa)	:	8.18000E+07
Yield Stress (kPa)	:	7.92000E+05
Hardening Constant (kPa)	:	5.10000E+05
Hardening Exponent	:	2.60000E-01
Strain Rate Constant	:	1.40000E-02
Thermal Softening Exponent	:	1.03000E+00
Melting Temperature (K)	:	1.79300E+03

FAILURE MODEL: None

EROSION MODEL: None

## C ANALYTICAL METHOD FOR JOINT IMPACTS

Here the analytical method applied to joint impacts is described. We define  $\mathbf{A}=\mathbf{A}(w,z)$  as the parametrised projectile surface, where  $z$  is along the projectile axis and  $w$  is the rotation angle. The variables are defined in Figure C.1. In terms of the ogive radius  $R_{ogive}$  and the projectile radius  $R_{proj}$  we can express  $\mathbf{A}$  in the following way:

$$\mathbf{A}(w,z) = [r(z)\cos w, r(z)\sin w, z]$$

$$r(z) = \sqrt{R_{ogive}^2 - z^2} - (R_{ogive} - R_{proj})$$

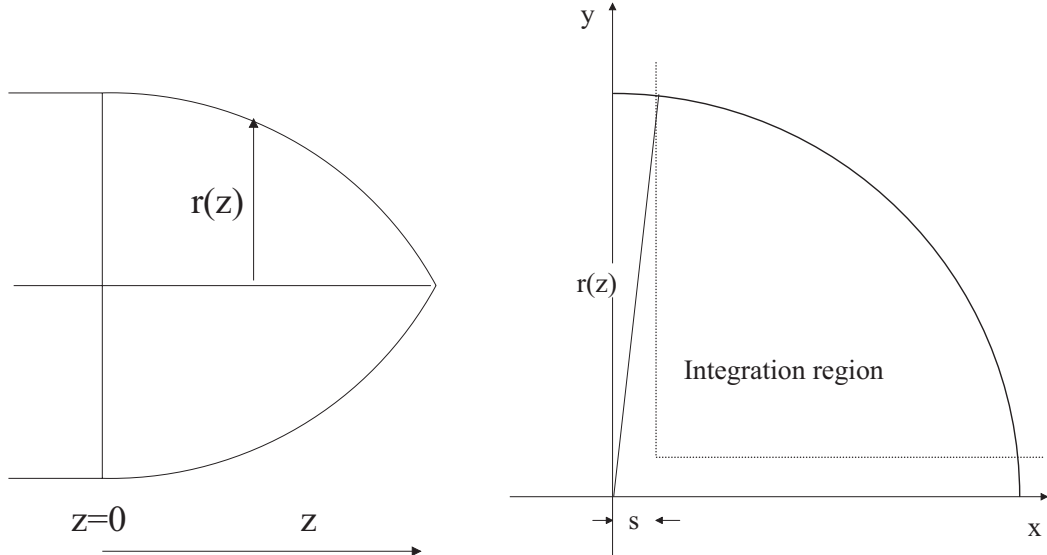


Figure C.1 Parametrisation of the projectile nose geometry.

Based on Figure C.1, the range of  $w$  is seen to be given by:

$$w_{\min} = \arcsin\left(\frac{s}{r(z)}\right)$$

$$w_{\max} = \frac{\pi}{2} - \arcsin\left(\frac{s}{r(z)}\right)$$

where  $2s$  denotes the separation between neighbouring concrete blocks. The integration limits of  $w$  thus depend on the value of  $z$ . The  $z$ -coordinate runs from zero at the base of the tip to the maximum value of

$$z_{\max} = \sqrt{{R_{ogive}}^2 - (\sqrt{2}s + (R_{ogive} - R_{proj}))^2}$$

The minimum value of  $z$  is zero if the projectile nose has penetrated fully into the target, otherwise it is  $z_{\max} - x$ , where  $x$  is the momentary penetration depth.

Using Equation (3.2), we can now express the force as

$$F_z = - \int_{z_{\min}}^{z_{\max}} \int_{w_{\min}}^{w_{\max}} p_r(v) \frac{z}{R_{ogive}} \left\| \frac{\partial \mathbf{A}}{\partial w} \times \frac{\partial \mathbf{A}}{\partial z} \right\| dw dz$$

which is identical to the expression for penetration into an infinite, solid block, except for the integration limits. Rewriting the normal component of the velocity as  $v_n = vz/R_{ogive}$ , and using  $p_r = S\sigma_c + \rho v^2$  for the pressure, we can simplify the force integral further:

$$F_z = S\sigma_c C_1 + \rho v^2 C_3$$

$$C_n = -4 \int_{z_{min}}^{z_{max}} \int_{w_{min}}^{w_{max}} \left( \frac{z}{R_{ogive}} \right)^n \left\| \frac{\partial A}{\partial w} \times \frac{\partial A}{\partial z} \right\| dw dz$$

The factor 4 enters because the integration is carried out over one quadrant only. The formula also includes the initial penetration phase, where only a part of the projectile has entered the target, provided the pressure function is still valid. In this case, the “constants”  $C_n$  depend explicitly on the current penetration depth  $x$ , although they are indeed constant when the projectile nose has completely entered the target.

It is straightforward to integrate with respect to the angle  $w$  analytically. However, the complicated  $z$ -dependence forces us to resort to numerical computation. *Mathematica* is well suited for such a computation, and the routine used to calculate the penetration depth is found in Appendix D.

## D THE *MATHEMATICA* ROUTINE

In case anyone should venture to use this routine, the following is important to note:

- The text printed in bold are inputs. The variables have obvious meanings.
- Exception 1: interpolationsteps. This variable is related to numeric integration of the equation of motion.
- Exception 2: ModuleSeparation is  $s$  as defined in Figure 3.5. In other words, half the actual separation should be entered.
- For some reason the results are bad for rare combinations of input. An example is shown here. DiameterProjectile should be 20 mm, but with exactly that value the result is wrong. Instead, we have used values close to 20 mm. Notice that the inputs here have no connection to this report whatsoever, they are only there as an example of when things may go wrong.

For the *Mathematica* illiterate: everything between  $(*$  and  $*)$  are comments. Everything else can be skipped, you only need to worry about the bold faced inputs.

```
(*SPHERICAL CAVITY EXPANSION.*)
Off[General::spell1]; (*TO AVOID ERROR MESSAGES FOR SIMILAR VARIABLE NAMES*)

(*INPUTS*)
OgiveRadius = 50; (*"in mm"*)
DiameterProjectile = 19.999; (*"in mm"*)

MassProjectile = 0.162; (*kg*)
ModuleSeparation = 0.0;
(*"in mm, half the actual separation"*)
```

```

CompressionalStrength = 48*10^6; (*"Compressional strength in Pa"*)
PoissonRatio = 0.25;
YieldStress = 2.73*10^8(*Pa*);
ShearModulus = 2.5*10^10(*Pa*);
DensityTarget = 2.44; (*g/cm^3*);
InitialVelocity = 400.0(*m/s*);
interpolationsteps = 0.001(*This constant is related to accuracy.
It determines the number of points used to calculate the initial \
penetration phase force.
Smaller values of this constant gives longer runtimes.
0.01 gives virtually the same as 0.001,
so there is little point in using a smaller value.*);

(*INITIALISATIONS : CALCULATE NUMEROUS CONSTANTS NEEDED LATER ON,
AND CONVERT TO PURE METRIC UNITS*)
ORad = OgiveRadius*10^(-3);
PRad = DiameterProjectile*10^(-3)/2;
dens = DensityTarget*10^3;
mass = MassProjectile/4;
alpha = ModuleSeparation*10^(-3);
tiplength = Sqrt[2*ORad*PRad - PRad^2];
zmax = Sqrt[ORad^2 - (Sqrt[2]*alpha + (ORad - PRad))^2];
forceOpen = tiplength - zmax;
A = 49.5*(CompressionalStrength/(10^6)) ^ (-0.43)*CompressionalStrength;

(*PARAMETRISATION :
FURTHER CALCULATIONS REQUIRE DEFINITION OF PARAMETRISATION IN TERMS OF \
THE VARIABLES z AND w. THUS,
THIS IS THE PARAMETRISATION OF THE PROJECTILE SURFACE*)
(*THE TIP RADIUS AS \
A FUNCTION OF DISTANCE z FROM TIP BASE*)

ls[z1_] := Sqrt[ORad^2 - z1^2] - (ORad - PRad);
s[w_, z_] := {ls[z]*Cos[w], ls[z]*Sin[w], z};

(*NOW WE DEFINE THE RANGES OF THE TWO VARIABLES,
THE ROTATION ANGLE w AND THE HEIGHT VARIABLE z*)

wmin[z2_] := ArcSin[alpha/ls[z2]];
wmax[z2_] := Pi/2 - ArcSin[alpha/ls[z2]];
(*zmax IS ALREADY DEFINED*)
zmin[x1_] := zmax - x1;

(*CALCULATIONS
CALCULATE THE JACOBIAN USED IN THE INTEGRATIONS*)

vec1[w_, z_] = D[s[w, z], w];
vec2[w_, z_] = D[s[w, z], z];
crss[w_, z_] = Cross[vec1[w, z], vec2[w, z]];
jacobi[w_, z_] = Sqrt[crss[w, z].crss[w, z]];
Clear[vec1, vec2, crss];

(*CALCULATE THE TIP SURFACE INTEGRALS OF THE NORMAL COMPONENT DURING THE \
ENTIRE PENETRATION PHASE, INCLUDING THE INITIAL PHASE*)

(*INTEGRATE SYMBOLICALLY WITH RESPECT TO w*)

innerint1[z_] = Integrate[z*jacobi[w, z]/ORad, {w, wmin[z], wmax[z]}];
innerint2[z_] = Integrate[z^3*jacobi[w, z]/ORad^3, {w, wmin[z], wmax[z]}];

```

```

(*INTEGRATE THE PORTION OF THE TIP INSIDE THE TARGET NUMERICALLY WITH
RESPECT \
TO z*)

Aint = Compile[
  {{init, _Real}, {endpoint, _Real}, {steps, _Real}},
  Table[{xtable,
    NIntegrate[innerint1[z], {z, zmin[xtable], zmax},
      PrecisionGoal -> 6, MaxRecursion -> 6,
      MinRecursion -> 0]}, {xtable, init, endpoint, steps}],
  {{zmin, _Real}}];
Bv2int = Compile[
  {{init, _Real}, {endpoint, _Real}, {steps, _Real}},
  Table[{xtable,
    NIntegrate[innerint2[z], {z, zmin[xtable], zmax},
      PrecisionGoal -> 6, MaxRecursion -> 6,
      MinRecursion -> 0]}, {xtable, init, endpoint, steps}],
  {{zmin, _Real}}];
l1 = Aint[0.0, zmax, interpolationsteps];
l1 = Append[
  l1, {zmax,
    NIntegrate[innerint1[z], {z, 0.0, zmax}, PrecisionGoal -> 6,
      MaxRecursion -> 6, MinRecursion -> 0]}];
l2 = Bv2int[0.0, zmax, interpolationsteps];
l2 = Append[
  l2, {zmax,
    NIntegrate[innerint2[z], {z, 0.0, zmax}, PrecisionGoal -> 6,
      MaxRecursion -> 6, MinRecursion -> 0]}];

(*"DEFINE INTERPOLATION FUNCTIONS THROUGH THE POINTS CALCULATED ABOVE, FOR \
BOTH CONSTANT TERMS. THESE FUNCTIONS ARE VALID THROUGH THE INITIAL \
PENETRATION PHASE."*)

Afunc = Interpolation[l1];
Bv2func = Interpolation[l2];

(*SOLVE THE DIFFERENTIAL EQUATION FOR v(x) AND FIND THE VELOCITY WHEN x =
zmax*)

initpen =
  NDSolve[{v[x]*v'[x] == -(A*Afunc[x] + dens*Bv2func[x]*v[x]^2)/mass,
    v[0.0] == InitialVelocity}, v, {x, 0.0, zmax}];
(*"NOW INSERT INTO ANALYTIC EXPRESSION OBTAINED FROM SOLVING THE PENETRATION \
ODE FOR A COMPLETELY PENETRATED NOSE, BUT IN A MODULAR TARGET"*)
vel0 = Evaluate[v[zmax]] /. initpen[[1]]; (*
  VELOCITY AT THE END OF THE INITIAL PENETRATION PHASE*)

c1 = l1[[Length[l1], 2]];
c2 = l2[[Length[l2], 2]];
pen = zmax + force0open + mass/(2*dens*c2)*Log[1 + dens*c2*vel0^2/(A*c1)];
pen*10^3

```



## DISTRIBUTION LIST

**FFIBM****Dato:** 27. juni 2003

RAPPORTTYPE (KRYSS AV)	<input checked="" type="checkbox"/> RAPP <input type="checkbox"/> NOTAT <input type="checkbox"/> RR	RAPPORT NR.	REFERANSE	RAPPORTENS DATO
X		2001/05787	FFIBM/766/130	12. December 2002
RAPPORTENS BESKYTTELSESGRAD		ANTALL TRYKTE UTSTEDT	ANTALL SIDER	
Unclassified		35	26	
RAPPORTENS TITTEL PENETRATION INTO MODULAR TARGETS		FORFATTER(E) OLSEN Åge Andreas Falnes, SJØL Henrik, TELAND Jan Arild		
FORDELING GODKJENT AV FORSKNINGSSJEF  Bjarne Haugstad		FORDELING GODKJENT AV AVDELINGSSJEF:  Jan Ivar Botnan		

**EKSTERN FORDELING****INTERN FORDELING**

ANTALL	EKS NR	TILOS	ANTALL	EKS NR	TILOS
1		Forsvarsbygg Oslo Mil/Akershus, 0015 Oslo	9		FFI-Bibl
1		v/Helge Langberg	1		FFI-ledelse
1		v/Leif Riis	1		FFIE
1		FortV SE-63189 Eskilstuna	1		FFISYS
1		v/Björn Lindberg	1		FFIBM
1		v/ Leif Ekblom	1		FFIN
2		Åge Andreas Falnes Olsen Fysisk institutt Universitetet i Oslo Postboks 1048 Blindern 0316 Oslo	4		Forfattereksemplar(er) Restopplag til Biblioteket
			5		
					<b>Elektronisk fordeling:</b> FFI-veven Eirik Svinsås (ESv) Bjarne Haugstad (BjH) Knut B Holm (KBH) Svein E Martinussen (SEM)